NASA TECHNICAL NOTE NASA TN D-3370

NASA TN D-3370

# A PARAMETRIC STUDY OF FACTORS INFLUENCING THE DEEP-STALL PITCH-UP CHARACTERISTICS OF T-TAIL TRANSPORT AIRCRAFT

*by Bruce G. Powers*

*Flight Research Center*
*Edwards, Calif.*

NATIONAL AERONAUTICS AND SPACE ADMINISTRATION • WASHINGTON, D. C. • AUGUST 1966

NASA TN D-3370

# A PARAMETRIC STUDY OF FACTORS INFLUENCING THE DEEP-STALL PITCH-UP CHARACTERISTICS OF T-TAIL TRANSPORT AIRCRAFT

By Bruce G. Powers

Flight Research Center
Edwards, Calif.

NATIONAL AERONAUTICS AND SPACE ADMINISTRATION

For sale by the Clearinghouse for Federal Scientific and Technical Information
Springfield, Virginia 22151 – Price $2.00

# A PARAMETRIC STUDY OF FACTORS INFLUENCING THE DEEP-STALL PITCH-UP CHARACTERISTICS OF T-TAIL TRANSPORT AIRCRAFT

By Bruce G. Powers
NASA Flight Research Center

## SUMMARY

An analog-computer program was conducted to study the factors influencing the deep-stall pitch-up characteristics representative of T-tail transport aircraft in a clean configuration with an aft center of gravity. Six pitching-moment curves were used and included variations of deep-stall as well as initial-stall pitching-moment characteristics. A stall maneuver with specified control rates was used, with deceleration rates into the stall of 1, 3, and 5 knots per second. The effects of gusts in causing pitch-up were also investigated. The study was limited to the three longitudinal degrees of freedom.

During a stall maneuver, the time available for a pilot to initiate an acceptable recovery was significantly reduced as the severity of the pitch-up in the deep-stall region was increased. A region of increased stability at the initial stall increased the time available before the pitch-up region was encountered and also provided an additional margin to prevent pitch-up due to gust penetration. If recovery from a stall maneuver was initiated as a function of angle of attack, the shape of the pitching-moment curve had only small effects on altitude losses during recovery.

## INTRODUCTION

With the recent introduction of several T-tail transport airplanes, there has been renewed interest in the pitch-up and/or stall characteristics of configurations with high horizontal tails. One aspect of the pitch-up problem is that of recovery from a pitched-up condition and the associated problem of avoiding the pitch-up region. Studies of longitudinal performance (refs. 1 to 3) have been concerned primarily with fighter-type aircraft in the transonic region. In these cases, the pitch-up usually occurred below the maximum lift coefficient, and the major concern was to avoid the pitch-up region in order to limit the angle of attack and, therefore, load factor. With the current T-tail transport configurations, the primary area of concern is the recovery from the pitch-up condition in the low-speed, high-angle-of-attack, or deep-stall, region. The limitation of angle of attack is not generally necessary from load considerations, since the loads are not increasing during a pitch-up in the stall region, with the possible exception of buffet loads.

As part of the NASA study (refs. 4 to 8) of various aspects of the deep-stall pitch-up problem, an analog-computer program was conducted at the NASA Flight Research Center, Edwards, Calif. This paper presents the results of the program, in which the relative effects of several parameters on the pitch-up characteristics of T-tail transport-type aircraft were investigated. A series of stall maneuvers was made with deceleration rates into the stall of 1, 3, and 5 knots per second, with recovery initiated over a range of angle of attack. The relative effects of the shape of the pitching-moment curves in the deep-stall region as well as in the initial-stall region were determined in terms of angle-of-attack overshoot and altitude losses during recovery. A series of stall maneuvers was also made with a deceleration rate of 3 knots per second to define the control moment required to recover from the deep-stall region at various levels of damping. The effect of the shape of the pitching-moment curve in preventing pitch-up due to gusts was investigated by using sine-wave gusts and recordings of continuous thunderstorm gusts.

## SYMBOLS

$a_n$ normal acceleration, g

$C_D$ drag coefficient, $\frac{\text{Drag}}{\bar{q}S}$

$C_L$ lift coefficient, $\frac{\text{Lift}}{\bar{q}S}$

$C_m$ pitching-moment coefficient, $\frac{\text{Pitching moment}}{\bar{q}S\bar{c}}$

$\Delta C_m$ incremental pitching-moment coefficient

$C_{m_q} = \frac{\partial C_m}{\partial\left(\frac{q\bar{c}}{2V}\right)}$

$C_{m_{\dot{\alpha}}} = \frac{\partial C_m}{\partial\left(\frac{\dot{\alpha}\bar{c}}{2V}\right)}$

$C_{m_{\delta_e}}$ elevator control effectiveness, $\frac{\partial C_m}{\partial \delta_e}$, per degree

$\bar{c}$ mean aerodynamic chord, feet

g acceleration due to gravity, feet per second$^2$

h altitude, feet

$\Delta h$ altitude loss, feet

| | |
|---|---|
| $I_Y$ | moment of inertia about the Y-axis, slug-foot$^2$ |
| q | pitching velocity, radians per second |
| $\bar{q}$ | dynamic pressure, pounds per square foot |
| S | wing area, square feet |
| T | thrust, pounds |
| t | time, seconds |
| $t_d$ | delay time, time from $\alpha = 15°$ to $\alpha_r$, seconds |
| $t_r$ | recovery time, time from $\alpha_r$ to $\alpha = 15°$, seconds |
| V | true velocity, feet per second |
| $V_e$ | equivalent velocity, knots |
| $V_s$ | equivalent stall speed based on maximum $C_L$, knots |
| W | airplane weight, pounds |
| $w_g$ | vertical gust velocity, feet per second |
| $\alpha$ | angle of attack, degrees |
| $\Delta\alpha$ | incremental angle of attack, degrees |
| $\alpha_g$ | incremental angle of attack due to gust velocity, degrees |
| $\alpha_{max}$ | maximum angle of attack attained during the stall maneuver, degrees |
| $\alpha_r$ | recovery angle of attack, degrees |
| $\gamma$ | flight-path angle, degrees |
| $\delta_e$ | elevator deflection, degrees |
| $\Theta$ | pitch angle, degrees |
| $\rho$ | air density, slugs per cubic foot |

A dotted quantity indicates a derivative with respect to time.

## TEST SETUP

An analog computer which mechanized the three longitudinal degrees of freedom was used for the tests. Simulated gusts were put into the computer as incremental angles of attack obtained from an analog-generated sine wave and from a continuous tape recording of thunderstorm gust velocities (ref. 9). The three-degree-of-freedom wind-axes equations of motion used were:

Pitch
$$\dot{q} = \frac{1}{2}\rho V^2\left(\frac{S\bar{c}}{I_Y}\right)\left[C_{m_{\delta_e}}\delta_e + C_m + \frac{\bar{c}}{2V}\left(C_{m_q}q + C_{m_{\dot{\alpha}}}\dot{\alpha}\right)\right]$$

Lift
$$\dot{\alpha} = q + \frac{g}{V}\cos\gamma - \frac{\rho g V}{2\left(\frac{W}{S}\right)}C_L - \frac{gT}{VW}\sin\alpha$$

Drag
$$\dot{V} = -g\sin\gamma - \frac{\rho g V^2}{2\left(\frac{W}{S}\right)}C_D + g\frac{T}{W}\cos\alpha$$

The following aircraft physical characteristics, which are representative of short-haul, transport-type aircraft, were assumed for this study:

$$\bar{c} = 13 \text{ ft}$$

$$\frac{W}{S} = 90 \text{ lb/sq ft}$$

$$\frac{S\bar{c}}{I_Y} = 0.01 \text{ ft/slug}$$

The aerodynamic coefficients $C_{m_{\delta_e}}$, $C_{m_q}$, $C_m$, $C_L$, and $C_D$ were programed as functions of angle of attack and are presented in figure 1. The pitching-moment curves are based on unpublished wind-tunnel data corresponding to an aft-center-of-gravity condition and cover a range of pitching-moment shapes that encompasses most T-tail transport configurations.

The pitching-moment curves A, B, C, and D shown in figure 1(a) were used to investigate the effects of pitching-moment shape in the deep-stall region. These curves covered the range from the linear, stable pitching-moment curve A, through the neutrally stable curves B and C, to the fairly severe pitch-up curve D. Curve B is neutrally stable with zero elevator but is slightly stable with the elevator trimmed at the initial stall angle of attack of 20°; whereas, curve C is slightly unstable with zero elevator and neutrally stable when trimmed at $\alpha = 20°$. Curves D, E, and F were included in the study to cover a range of initial stall variations in pitching-moment shape. The curves range from a destabilizing tendency (curve E) to a stabilizing tendency (curve F). The basic control effectiveness is shown in figure 1(b) and was used with elevator deflection limits of 15° to -25°, which provided a pitch-down capability throughout the angle-of-attack range for all of the pitching-moment curves.

Variations of the basic control effectiveness were used to determine the pitching-moment requirements for recovery from the deep-stall region. Figure 1(c) shows the variations and the total pitch down $C_m$ available for the various values of control effectiveness.

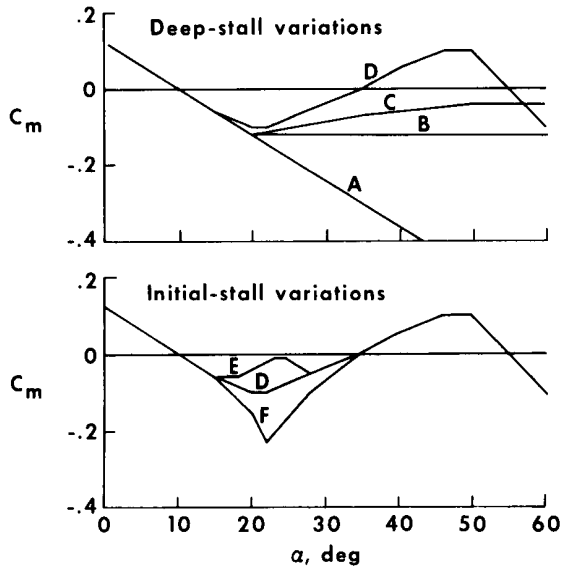


(a) Pitching-moment characteristics; $\delta_e = 0°$.

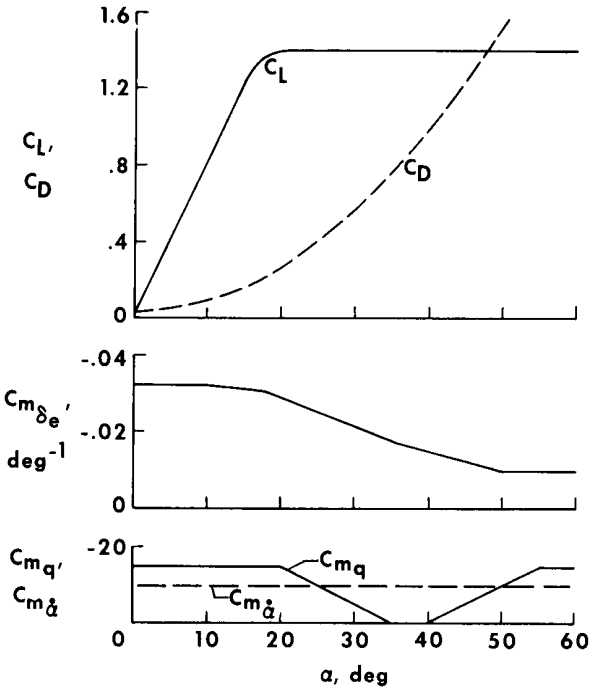


(b) Lift, drag, control, and damping characteristics.

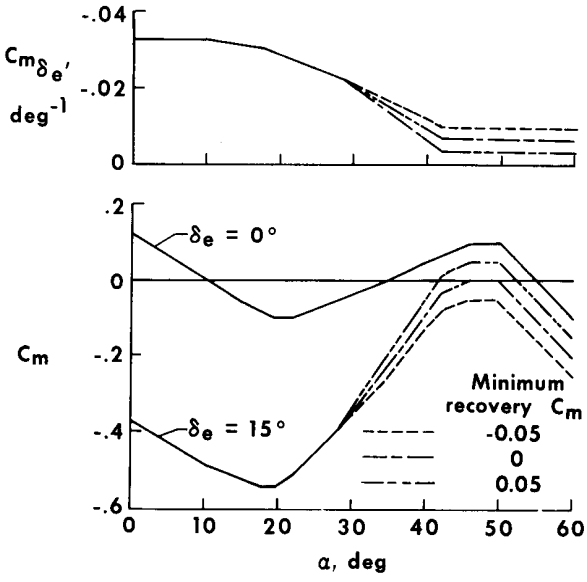


(c) Control-effectiveness characteristics used for determining recovery pitching-moment requirements.

Figure 1.— Aerodynamic characteristics.

## TEST MANEUVERS

The basic test maneuver was a conventional stall-demonstration maneuver. Typical time histories of the test maneuver are shown in figures 2(a) and 2(b). To provide a precise comparison of the various pitching-moment characteristics, a well-defined maneuver based on flight experience was used. The maneuver consisted of a zero-thrust deceleration at either 1, 3, or 5 knots per second from a speed of 175 knots. The elevator control rate was varied to maintain the desired deceleration and was approximately constant until recovery was initiated at a predetermined angle of attack. For recoveries initiated at angles of attack above that for the initial stall, the control rate was held constant at the value existing at the initial stall. ("Initial stall," as used herein, refers to the first point of maximum $C_L$ at $\alpha = 20°$.) Thrust was applied at recovery initiation with a 3-second engine time constant to give a thrust-to-weight ratio of 0.25. To minimize the angle-of-attack undershoot when returning to the trim condition, the recovery control input was maintained until zero pitch angle was reached. At that point, the recovery control input was reduced until zero pitch rate was obtained, which usually occurred at a pitch angle of -10° to -20°. Trim speed was then regained and a pullup to level flight was performed using a 2.5 load-factor limit. Recovery was considered to be complete when level flight was achieved. The control rates used in the maneuver were approximately 5 degrees per second with the exception of the stall entry portion, which ranged from 0.1 degree per second to 0.5 degree per second, depending on the deceleration rate.

The basic stall maneuver is characteristic of a flight situation in which the pilot does not recognize the stall condition until he is into the deep-stall region. An alternate situation could also exist in which the pilot misinterprets the stall condition, for example, noting a decrease in normal acceleration and then pulling up farther into the stall in an attempt to regain 1g flight. This situation was represented by a stall maneuver with a deceleration rate of 3 knots per second and a rapid pitch-up control input of 5 degrees per second at the initial stall ($\alpha = 20°$), which was continued until recovery initiation. The recovery remained the same as for the basic maneuver. A typical time history of this alternate maneuver is shown in figure 2(c).

In evaluating the stall maneuver, the following parameters, which are illustrated in figure 2, were found to be useful. The delay time $t_d$ is defined as the time from $\alpha = 15°$ to $\alpha_r$. The term represents the amount of time that the recovery initiation was delayed past an assumed stall warning at $\alpha = 15°$. The recovery time $t_r$ is the time required to return to $\alpha = 15°$ from recovery initiation and is an indication of the length of time spent in the stall region. Altitude loss $\Delta h$ is the total altitude lost from the start of the maneuver to the completion of the recovery (level flight). The maximum angle of attack attained during the maneuver $\alpha_{max}$ is a measure of the overshoot ($\alpha_{max} - \alpha_r$) and may also be indicative of possible problems with lateral-directional stability and buffet loads.

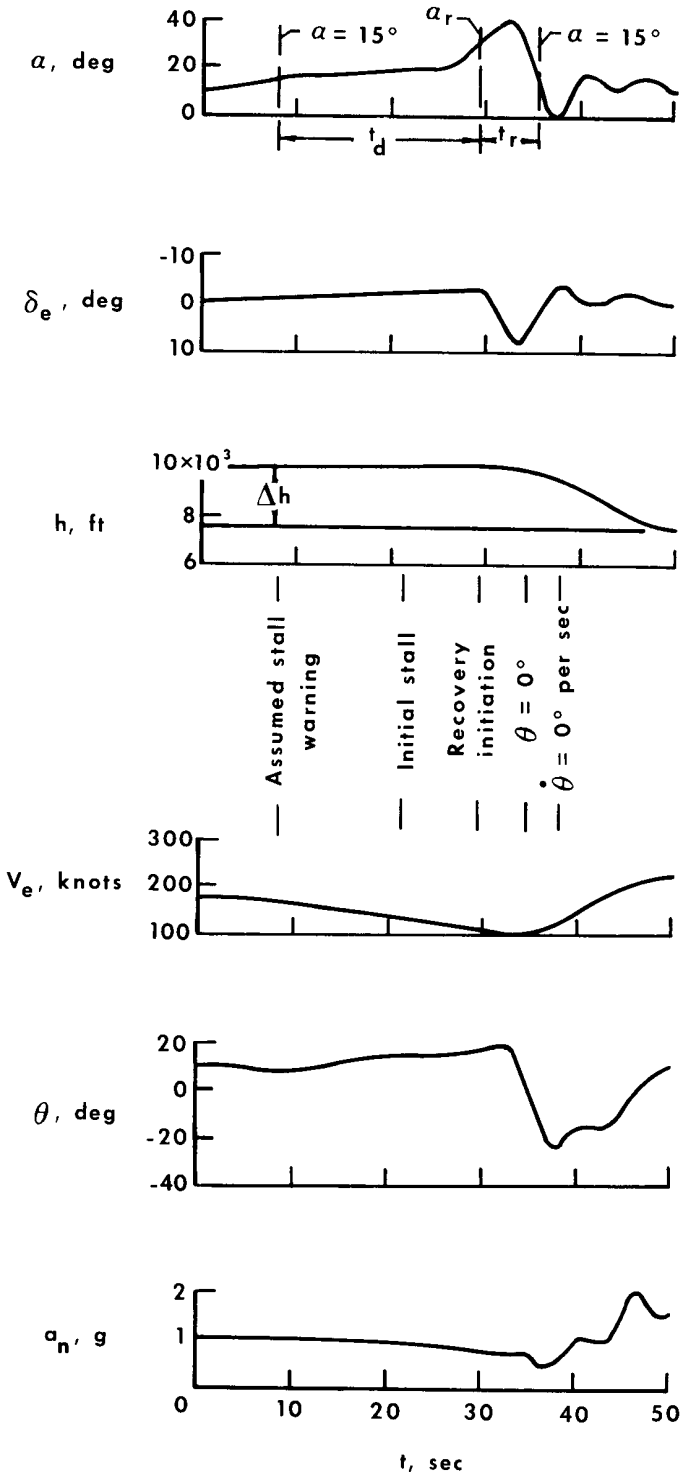


(a) Basic test maneuver with pitching-moment curve D.

Figure 2.– Typical time histories of stall maneuver.

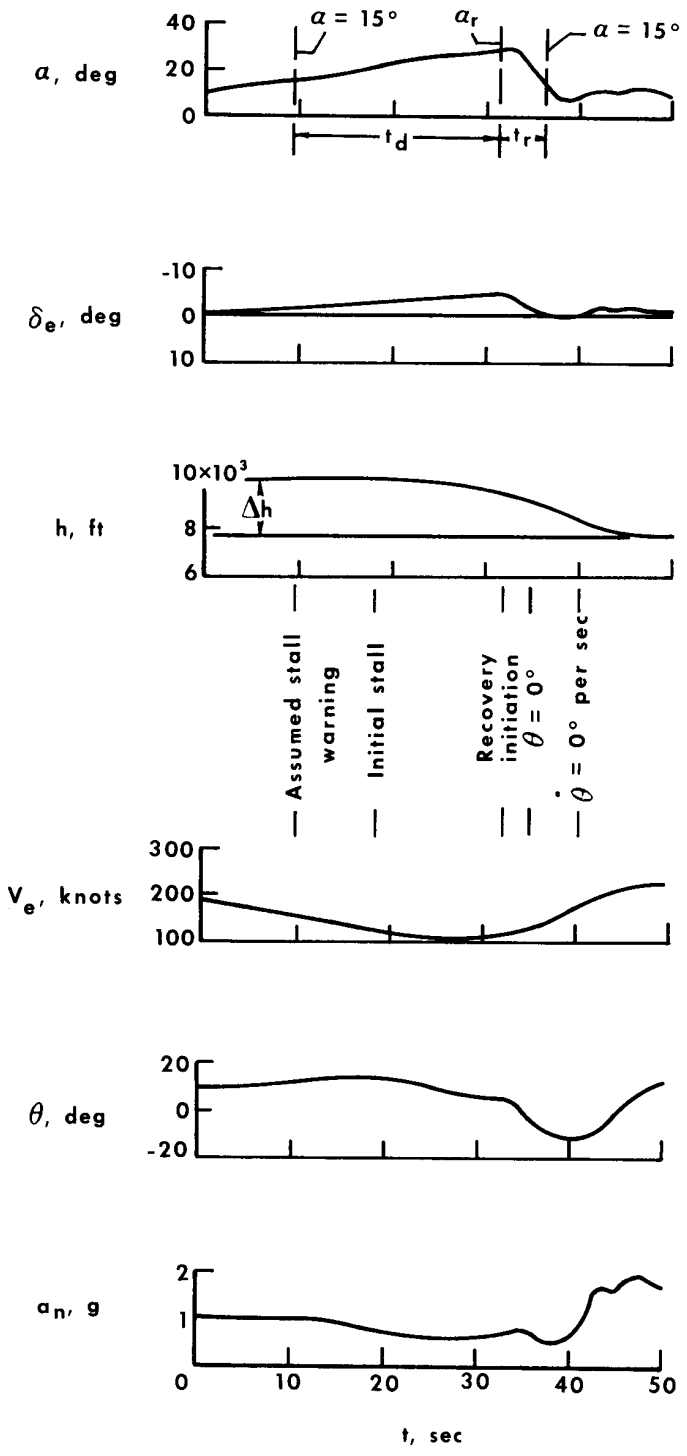


(b) Basic maneuver with pitching-moment curve A.

Figure 2.– Continued.

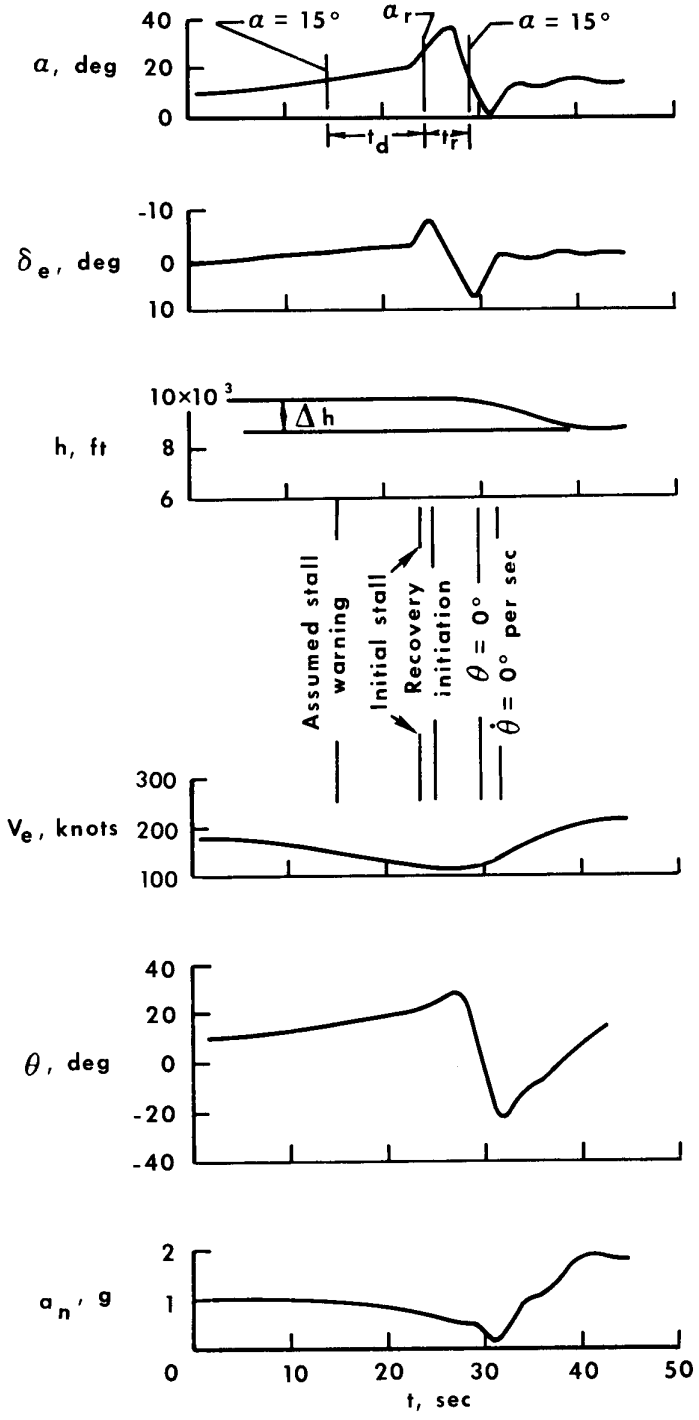


(c) Alternate maneuver with pitching-moment curve D.

Figure 2.– Concluded.

## RESULTS AND DISCUSSION

### Basic Data

The results for each of the six pitching-moment curves using the basic maneuver are shown in figures 3(a) to 3(f) in terms of $\alpha_{max}$, $\Delta h$, $t_d$, and $t_r$ as functions of the recovery initiation angle of attack $\alpha_r$ for deceleration rates into the stall of 1, 3, and 5 knots per second. These results would be useful in evaluating a situation in which there was a definite indication of the stalled condition, such as definite buffet or a mechanical indication such as a stick pusher, which would require recovery initiation to be made at a given angle of attack.

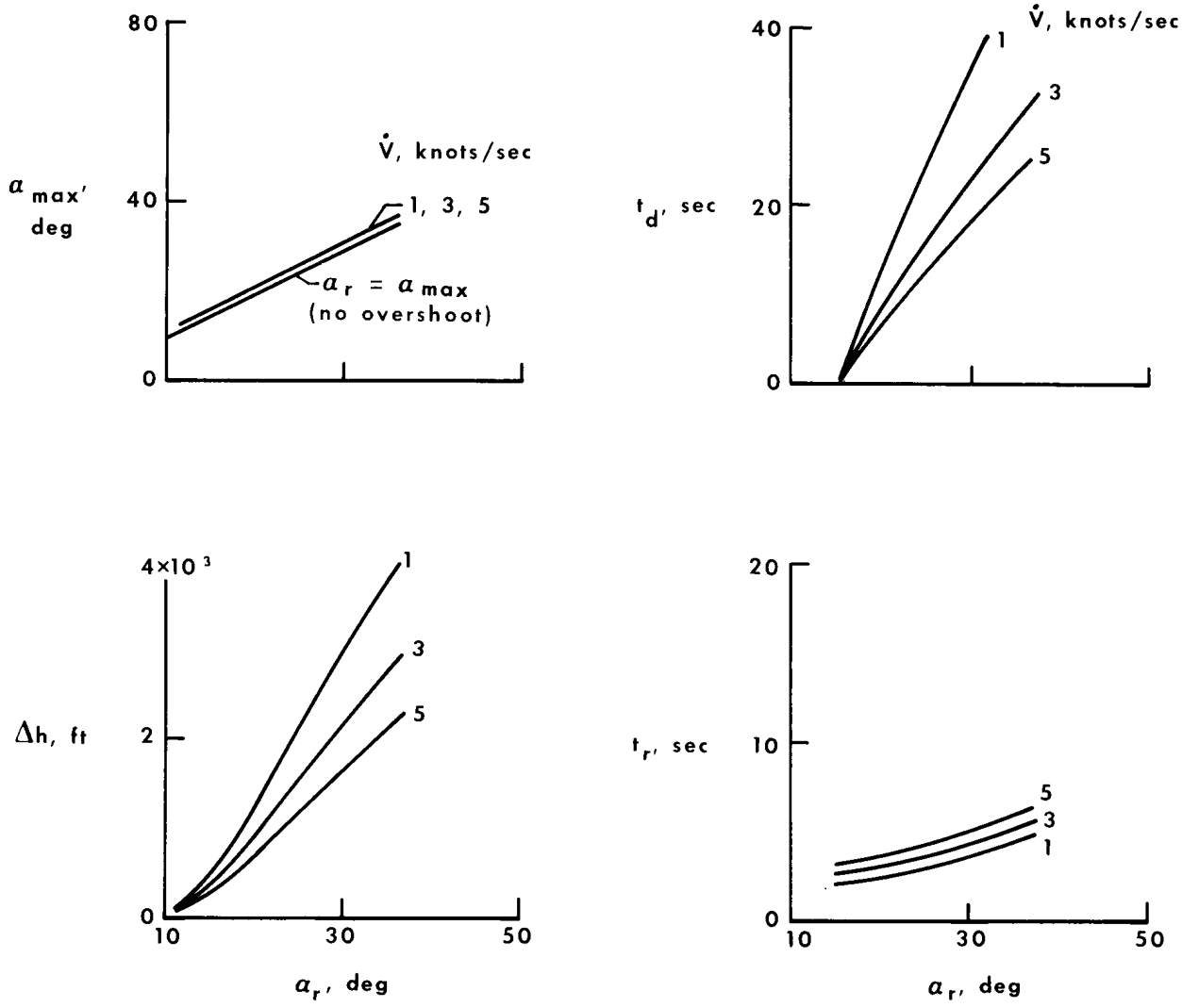


(a) Pitching-moment curve A.

Figure 3.– Effect of recovery-initiation angle of attack using the basic stall maneuver with entry rates of 1, 3, and 5 knots per second.

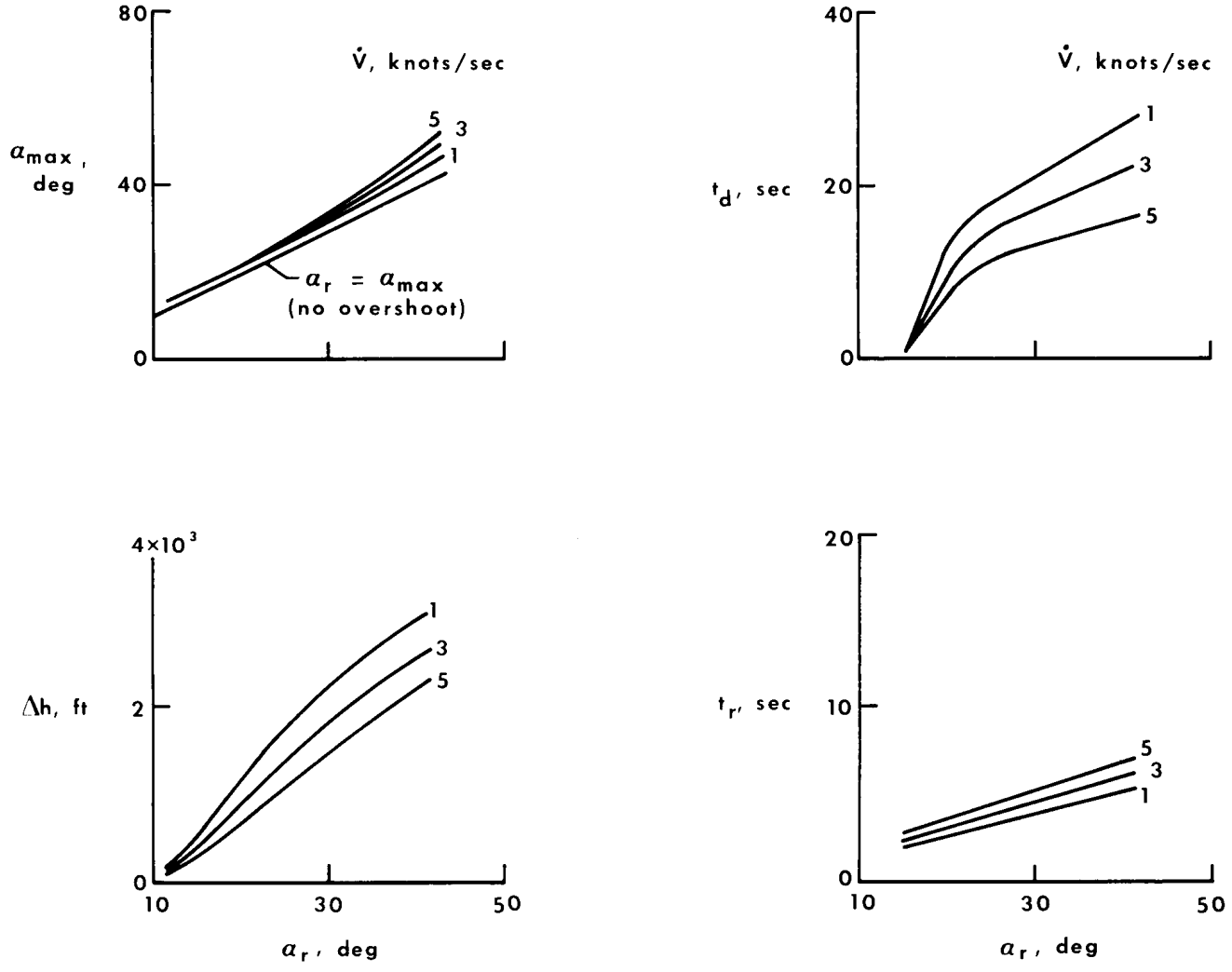


(b) Pitching-moment curve B.

Figure 3.– Continued.

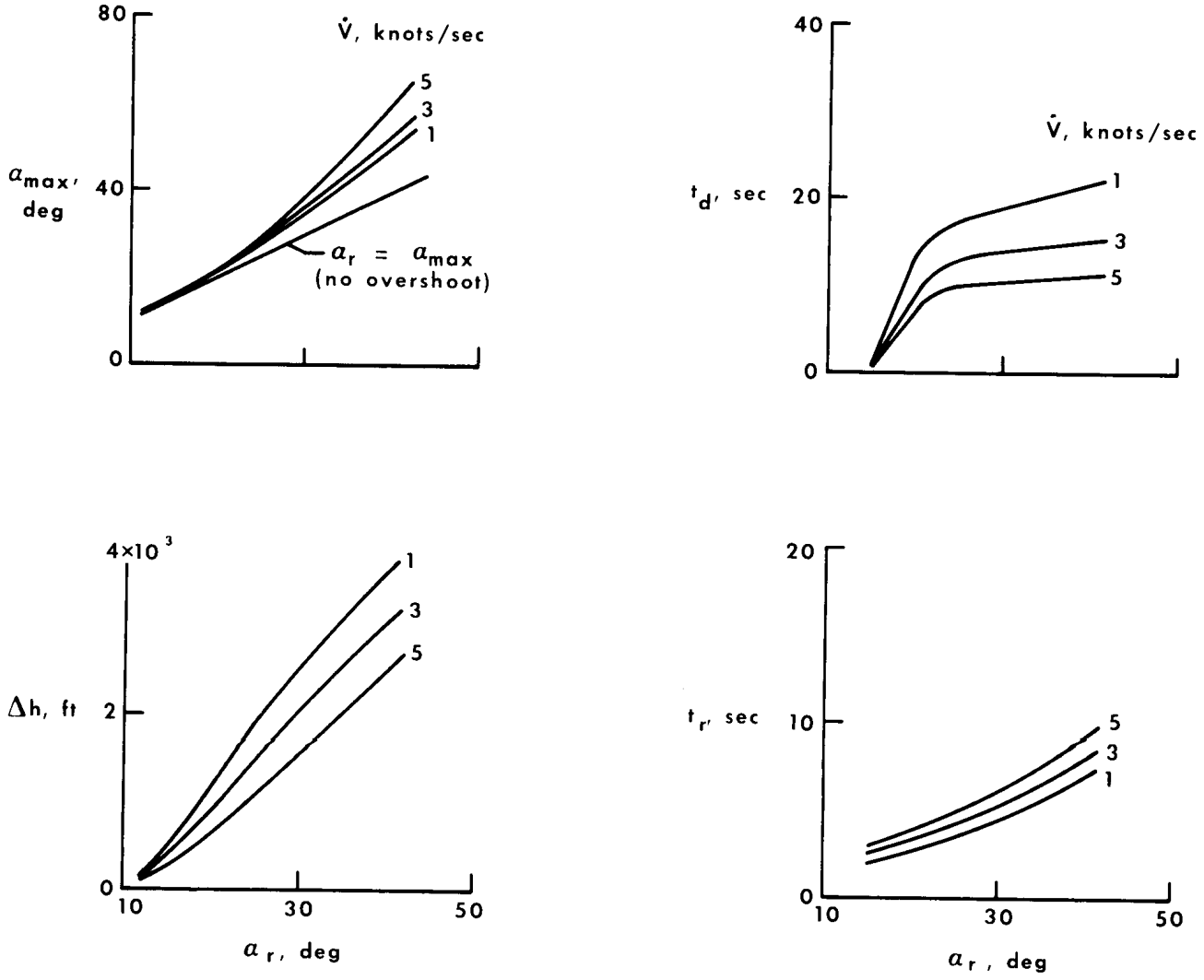


(c) Pitching-moment curve C.

Figure 3.– Continued.

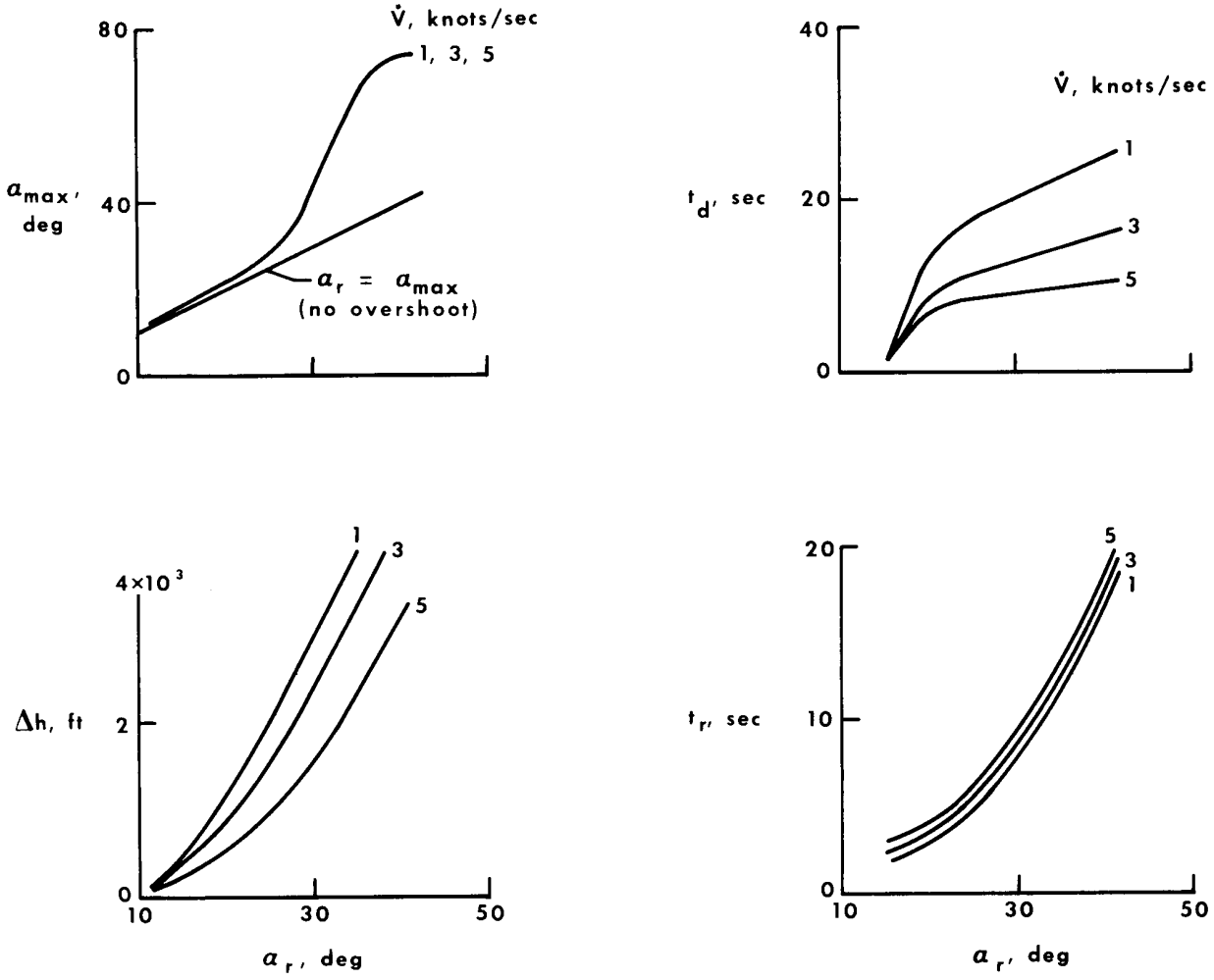


(d) Pitching-moment curve D.

Figure 3.– Continued.

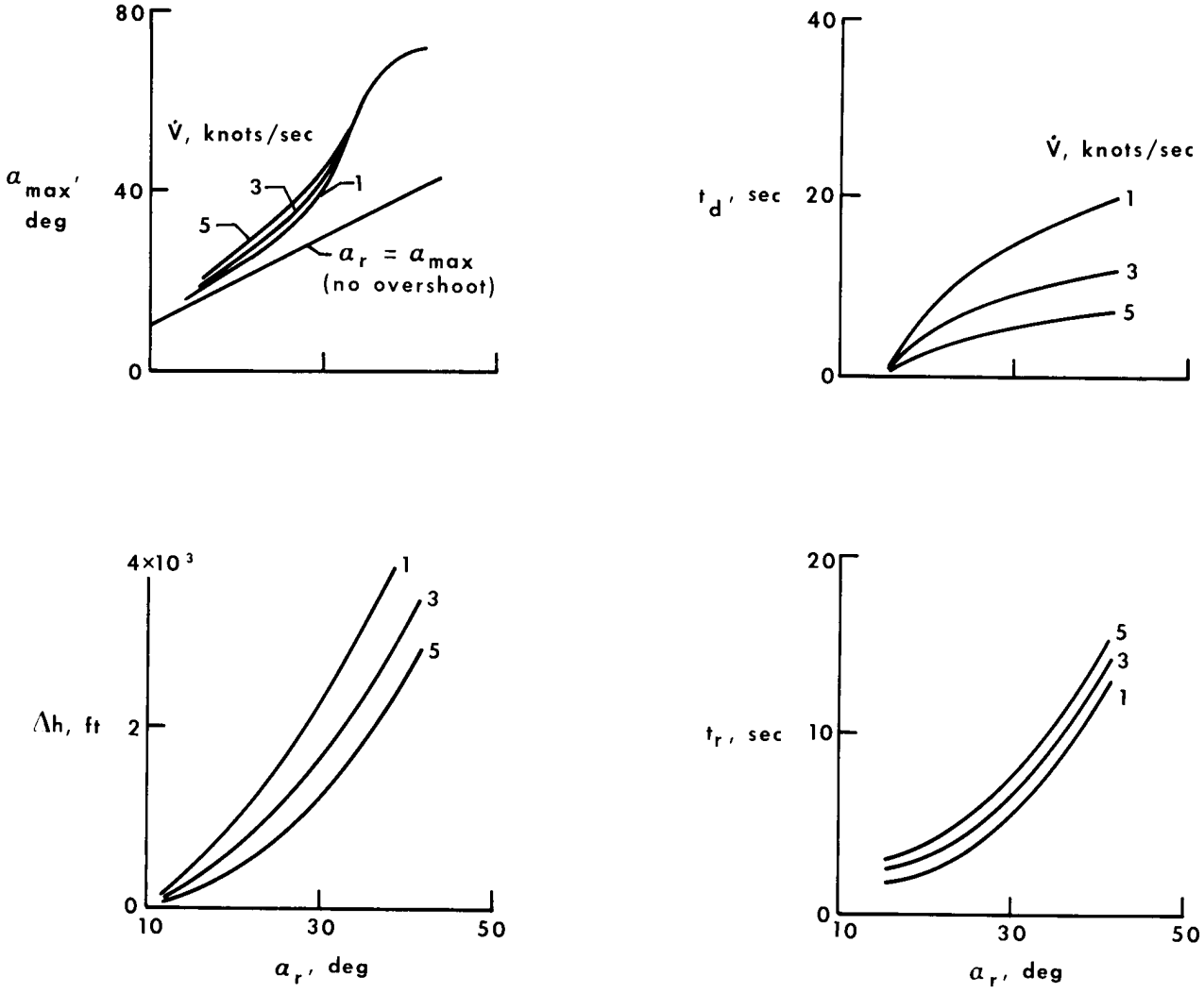


(e) Pitching-moment curve E.

Figure 3.– Continued.

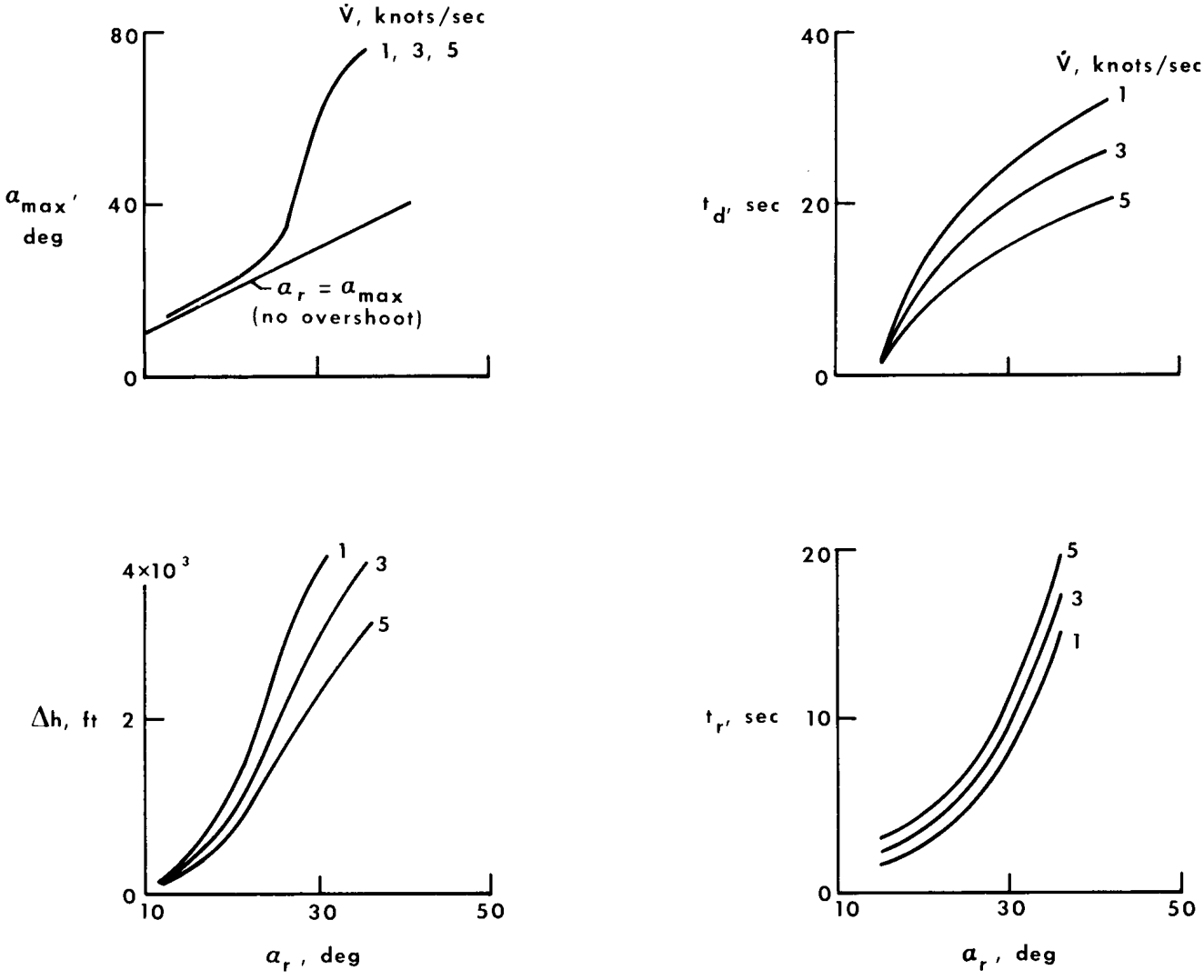


(f) Pitching-moment curve F.

Figure 3.– Concluded.

In order to consider the results from a second point of view, the data of figure 3 were replotted in figures 4(a) to 4(f) in terms of $\alpha_{max}$ and $\Delta h$ as a function of the delay time $t_d$. These results would be useful when there is no definite stall warning, so that the time available for the pilot to recognize the stalled condition is an important factor.

As the deceleration rate into the stall is increased, a small increase in recovery time is noted, which would tend to increase altitude losses (fig. 3); however, this tendency was compensated for by a large reduction in the time between stall warning and recovery initiation $t_d$. This reduction resulted in smaller altitude losses for the faster rates. For recovery based on the time factor $t_d$ (fig. 4), deceleration rate

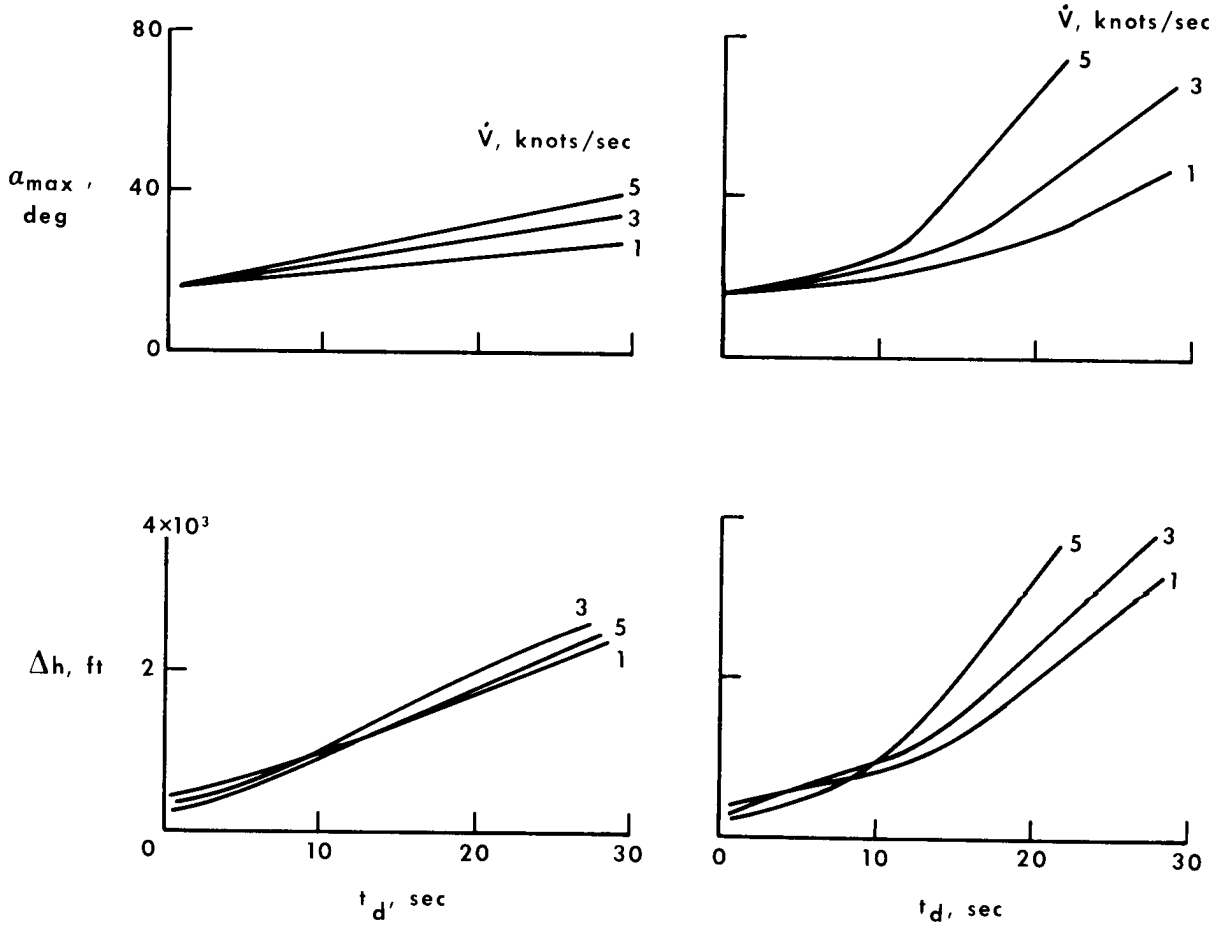


(a) Pitching-moment curve A.

(b) Pitching-moment curve B.

Figure 4.– Effect of delay time using the basic stall maneuver with entry rates of 1, 3, and 5 knots per second.

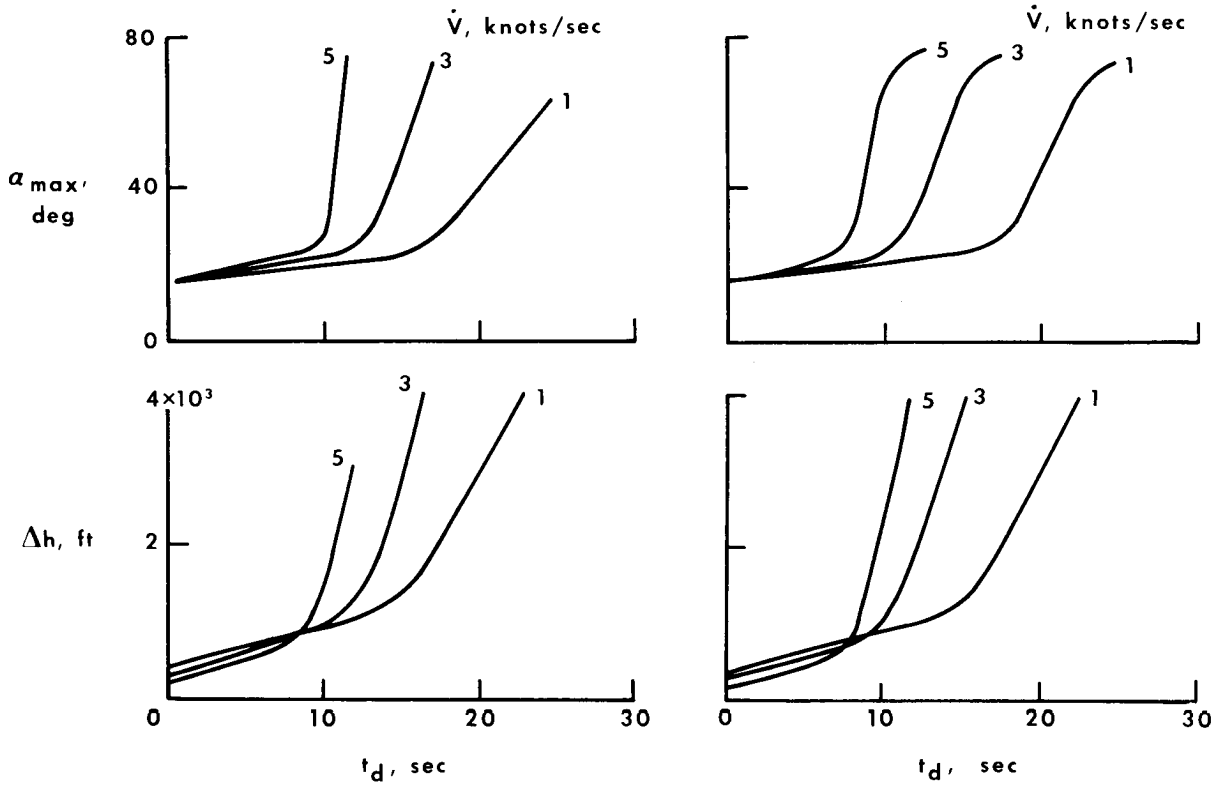


(c) Pitching-moment curve C.

(d) Pitching-moment curve D.

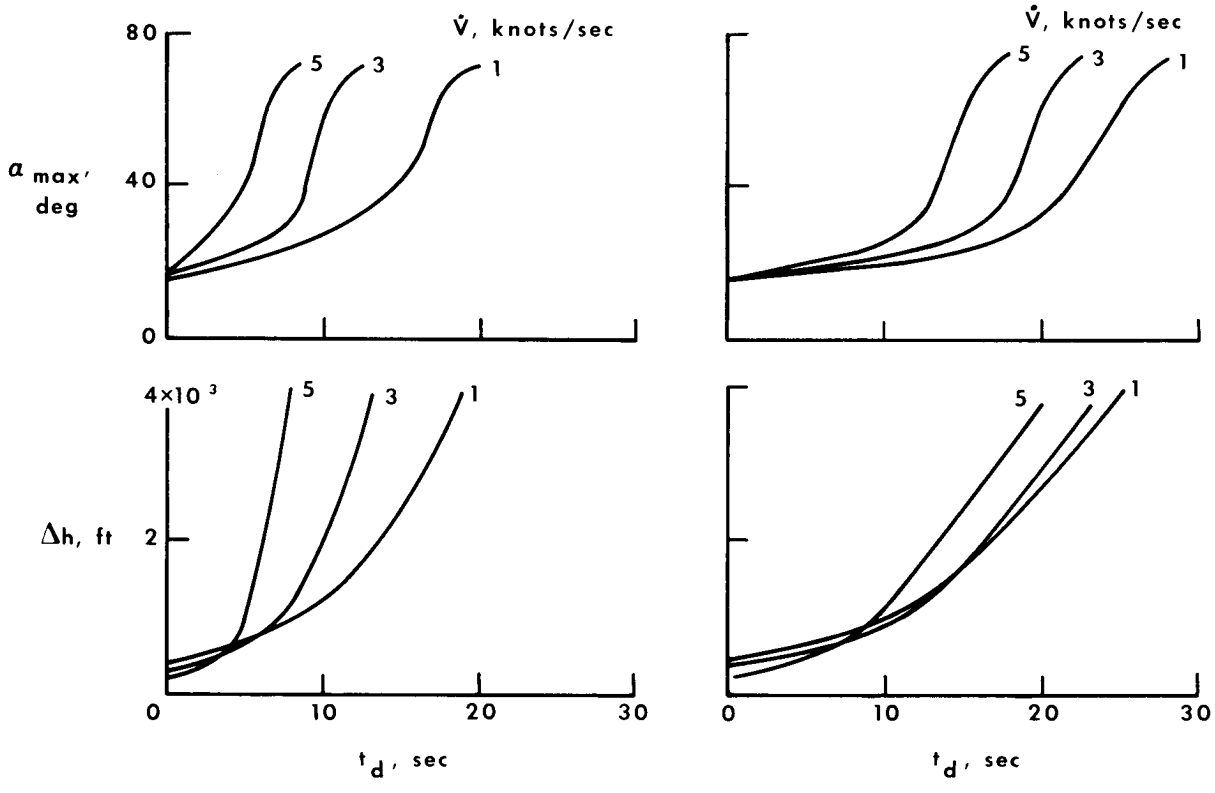


(e) Pitching-moment curve E.

(f) Pitching-moment curve F.

Figure 4.– Concluded.

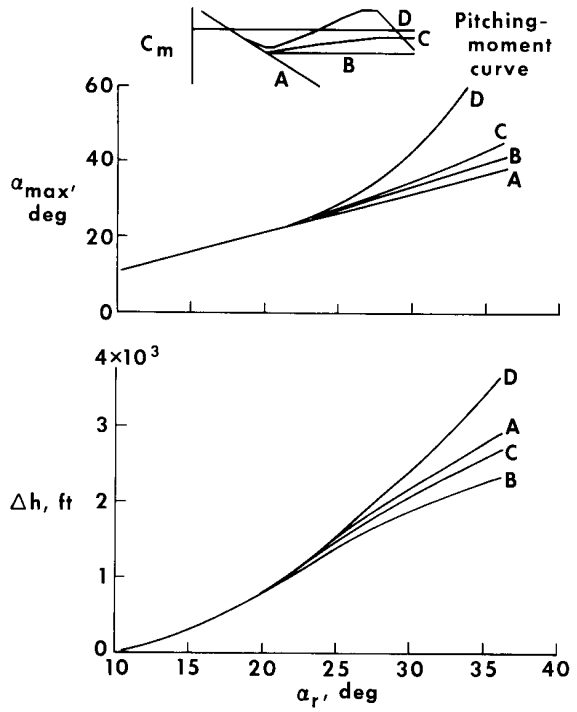


Figure 5.– Effect of deep-stall pitching-moment characteristics on angle-of-attack overshoot and altitude loss during recovery for recovery initiated as a function of angle of attack. Entry rate = 3 knots per second.

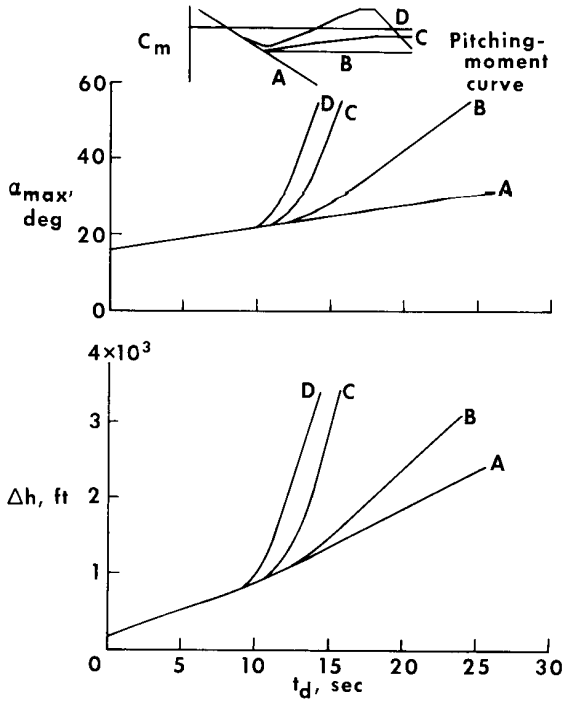


Figure 6.– Effect of deep-stall pitching-moment characteristics on angle-of-attack overshoot and altitude loss during recovery for recovery initiated as a function of time past a stall warning. Entry rate = 3 knots per second.

had almost no effect on altitude loss for the linear, stable curve (curve A). For the decreased stability curves, the higher rates reduced the time before a pitch-up occurred, which resulted in greater angle-of-attack overshoot and altitude loss at a given delay time. In general, the deceleration rate into the stall had little effect on the severity of the pitch-up for recoveries initiated as a function of angle of attack but could have a noticeable effect for recoveries initiated as a function of the time past a stall warning.

## Evaluation of Pitching-Moment Shape

Deep-stall characteristics. – To illustrate the effects of the shapes of the pitching-moment curves in the deep-stall region of $\alpha = 20°$ to $\alpha = 50°$, figures 3 and 4 are summarized in figures 5 and 6 for an entry rate of 3 knots per second. For recovery initiated as a function of angle of attack (fig. 5), there is no significant difference in either angle-of-attack overshoot or altitude loss for recoveries initiated at an angle of attack less than 25° (5° past the initial stall). Beyond $\alpha_r = 25°$, however, curve D shows a noticeable pitch-up and an associated large altitude loss as a result of long recovery times ($t_r$ in fig. 3). The linear pitching-moment curve, curve A, which might be expected to have the smallest altitude loss at a given $\alpha_r$, because of the low recovery time, has a relatively large altitude loss because of the longer time required to reach a given angle of attack. For curve B, pitch-up occurs relatively easily (low $t_d$) but recovery is also relatively easy (low $t_r$), resulting in the lowest altitude loss of the four pitching-moment curves.

A comparison of the maximum angle-of-attack and altitude loss of these same pitching-moment curves for the recovery initiation based on the time factor $t_d$ is shown in figure 6. As the level of deep-stall stability is increased, there is an

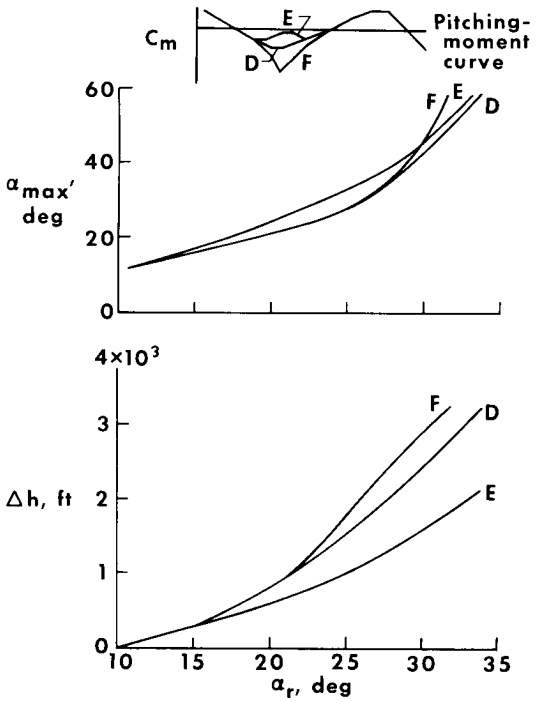


Figure 7.– Effect of pitching-moment characteristics at stall on angle-of-attack overshoot and altitude loss during recovery for recovery initiated as a function of angle of attack. Entry rate = 3 knots per second.

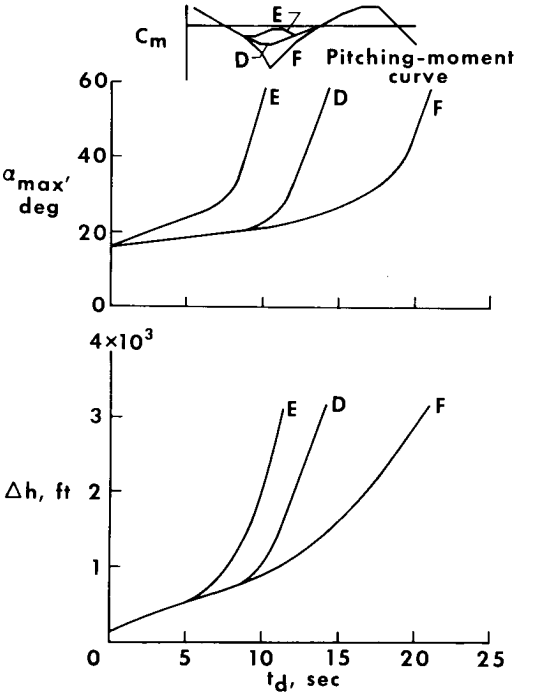


Figure 8.– Effect of pitching-moment characteristics at stall on angle-of-attack overshoot and altitude loss during recovery for recovery initiated as a function of time past the stall warning. Entry rate = 3 knots per second.

increase in the time required to reach a given value of $\alpha_{max}$ and, thereby, a reduction in the altitude loss for a given delay time. A significant difference in altitude loss occurs between curve C (neutrally stable when trimmed at the initial stall) and curve B (slightly stable when trimmed at the initial stall). It appears that if there is some degree of stability in the deep-stall region, altitude losses will be on the same order as those for a linear pitching-moment curve for a recovery initiated at the same delay time $t_d$. Similarly, neutral and unstable pitching-moment curves will have significantly larger altitude losses than the linear curve if recovery is not initiated until after the initial stall.

Initial-stall characteristics.– The effects of the pitching-moment characteristics in the initial-stall region on the maximum angle of attack and altitude loss are shown in figures 7 and 8. When recovery is initiated as a function of angle of attack (fig. 7), curve E, with the destabilizing tendency in the initial-stall region, shows less altitude loss than either curves D or F, with the moderate and highly stabilized regions at the initial stall, although the angle-of-attack overshoot is as much as 5° greater for the lower $\alpha_r$ recoveries. The detrimental effect of the stabilizing region on altitude losses for recoveries based on angle of attack is the result of the longer time required to reach a given angle of attack, due to the increased stability when entering the stall, combined with a greater recovery time, due to a more severe pitch-up caused by the greater degree of instability in the pitch-up region.

In terms of the time factor $t_d$, however, a progressive delay in pitch-up is noted as the stabilizing tendency at the initial stall is increased (fig. 8), which results in a reduction in altitude loss for a given delay time. These results were obtained with constant control-input rates, which did not include any rapid control inputs prior to recovery. For this type of

gradual entry into the stall region, a stabilizing tendency in the initial stall region can provide a significant delay in the occurrence of pitch-up. This delay would provide greater time in the buffet or other stall-warning region. With the increase in stability, there is also an increase in control forces. Both of these factors provide cues that aid the pilot in recognizing the stall condition and afford him additional time to initiate recovery. In figure 9 the trim-force requirements for pitching-moment curves D, E, and F are compared; a constant control-force gradient of 4 pounds per degree of elevator angle is assumed. As shown, curve F requires a force 19 pounds greater than curve D and 26 pounds greater than curve E before an unstable region in the pitching-moment curve is encountered. For a forward-center-of-gravity configuration, the trim elevator angle and force requirements will approximately double, making it difficult for the pilot to inadvertently pull up into the pitch-up region with the initial increased stability region of curve F.

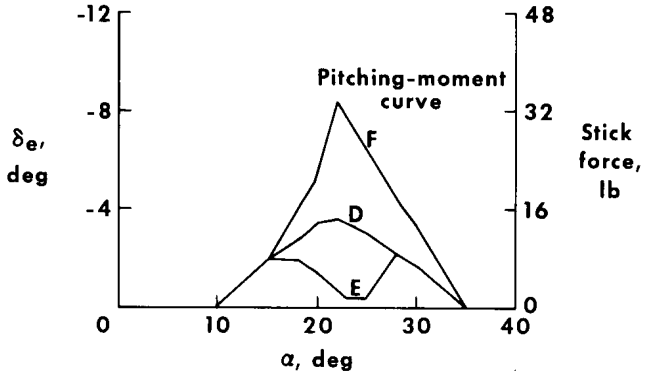


Figure 9.— Trim elevator angle and control column force required for three initial-stall pitching-moment characteristics.

Entry maneuver with alternate control inputs. — The alternate control maneuver shown in figure 2(c), with the pitch-up elevator input at $\alpha = 20°$ to simulate an inadvertent pilot input at the initial stall, was used with the pitching-moment curves with the deep-stall variations. The results are shown in figures 10(a) and 10(b). Included in figure 10(b) are the basic

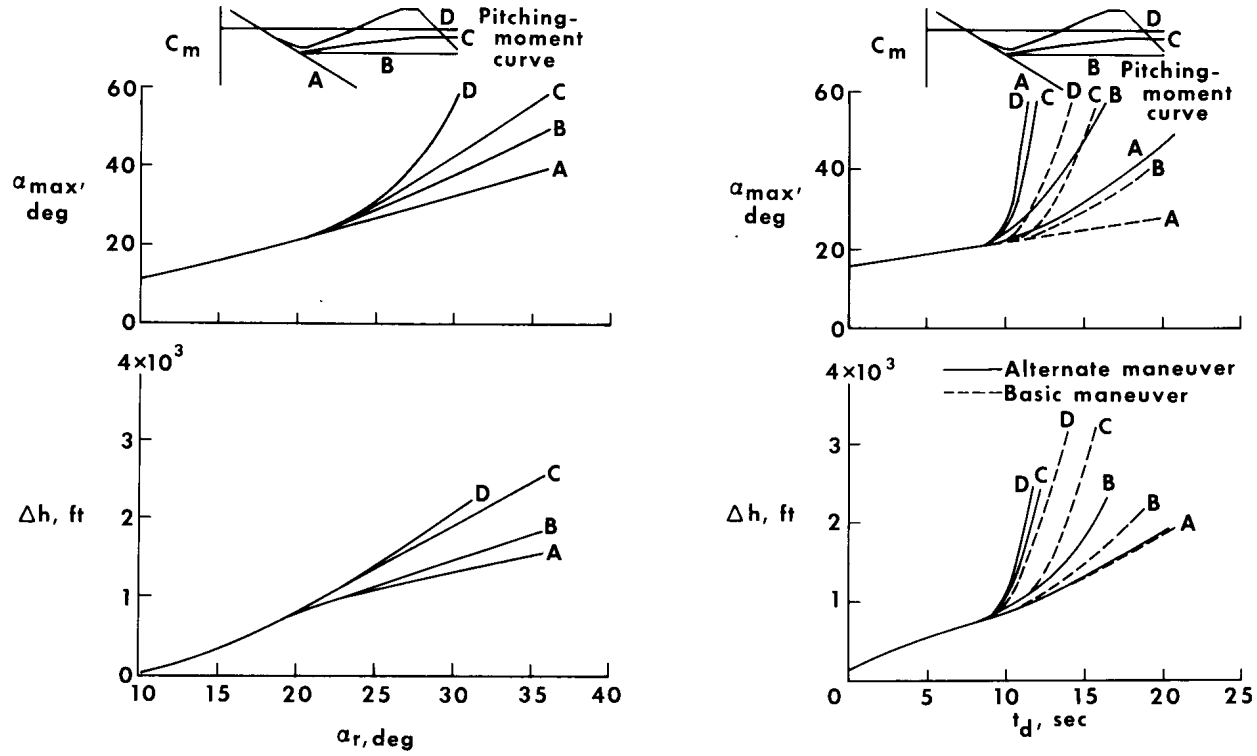


(a) As a function of recovery-initiation angle of attack.

(b) As a function of time past a stall warning.

Figure 10.— Effect of pitching-moment characteristics for entry rate of 3 knots per second using the alternate control maneuver with pitch-up control input at $\alpha = 20°$.

maneuver results of figure 6. The results follow the same trend as those with the basic maneuver except that the increase in altitude losses due to the longer delay times of curve A is no longer a significant factor, since the rapid pullup reduces the delay time to an extent that the altitude losses are primarily a function of recovery times (fig. 10(a)). The data again indicate that some degree of positive stability in the deep-stall region significantly decreases the angle-of-attack overshoot and altitude loss as a function of delay time (fig. 10(b)) and also, to some extent, as a function of recovery angle of attack.

The alternate control maneuver was also used with the pitching-moment curves with the initial stall variations. The results are shown in figures 11(a) and 11(b). The basic-maneuver data of figure 8 are included in figure 11(b). The results show the same trends as shown by the basic-maneuver data; however, the effectiveness of curve F in increasing the time before the pitch-up is encountered has been reduced, since the stabilizing region is passed through more rapidly as a result of the pitch-up control input.

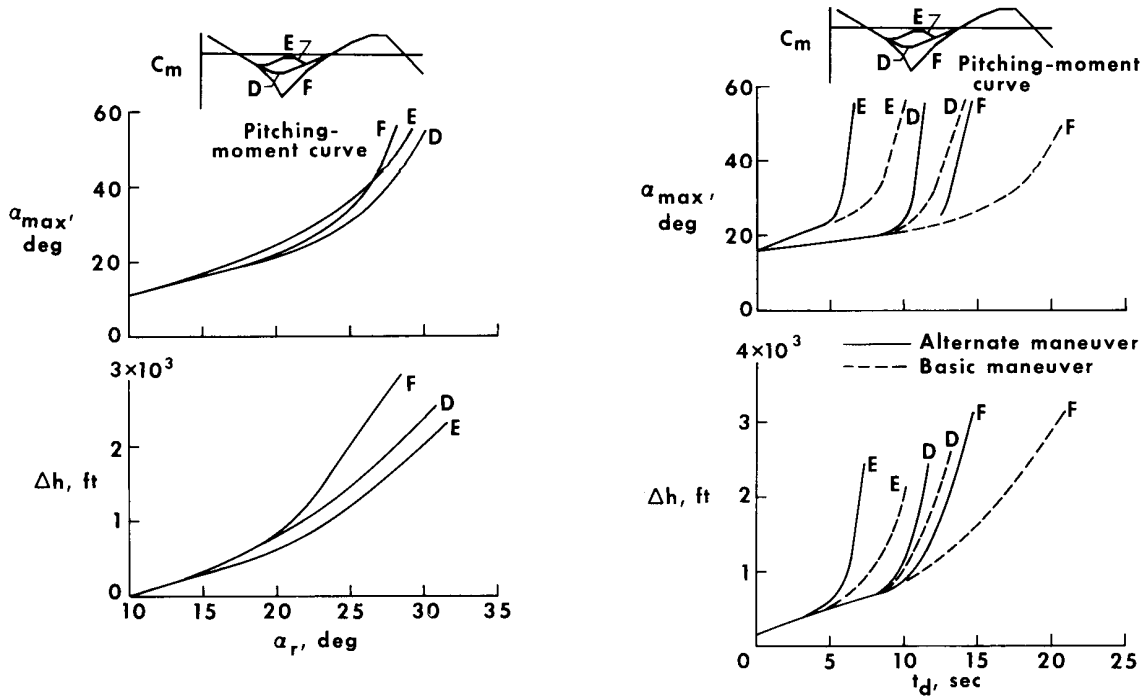


(a) As a function of recovery-initiation angle of attack.

(b) As a function of time past a stall warning.

Figure 11.– Effect of pitching-moment characteristics at stall for an entry rate of 3 knots per second using the alternate maneuver with pitch-up control input at $\alpha = 20°$.

## Pitching Moment Required for Recovery

With the pitching-moment characteristics of curve D, there is a possibility of retrimming in the deep-stall region. However, in the initial phases of the program, it was difficult to achieve a deep-stall retrim with the aerodynamic damping characteristics used because of the dynamics of the maneuver. When the deep stall was entered, pitching velocity was sufficient to make it possible to proceed well into the stable region at an angle of attack of about 50° to 60°, which resulted in a large pitch-down moment. This moment, combined with the light damping in that region, produced

sufficient nose-down pitching velocity to enable the airplane to pass through the deep-stall retrim region and return to the trim point at an angle of attack of 10°. Consequently, a series of stall maneuvers was made with various levels of damping (assumed constant with angle of attack) and control effectiveness (fig. 1(c)) to determine the pitching moment necessary to recover from the basic stall maneuver of figure 2 over a range of recovery-initiation angles of attack.

The results of these stall maneuvers, presented in figure 12, indicate the conditions that will produce a nonrecoverable deep-stall retrim in terms of recovery-initiation angle of attack and the incremental pitching moment available. The incremental pitching moment represents the minimum pitching moment available in the deep-stall region. With minimum damping $\left(C_{m_q} = -15,\ C_{m_{\dot{\alpha}}} = -10,\ \text{fig. 12(a)}\right)$, there is only a small region in which the maneuver produces a nonrecoverable retrim condition. As the damping increases, the nonrecoverable retrim region becomes larger (fig. 12(b)), but it is not until the damping is increased to $C_{m_q} = -60$ and $C_{m_{\dot{\alpha}}} = -45$ (fig. 12(c)) that the minimum pitching moment available must be in the nose-down direction for recovery. Thus, with the light damping usually present in the deep-stall region, recovery should always be possible if a slightly nose-down pitching moment is available throughout the deep-stall region.

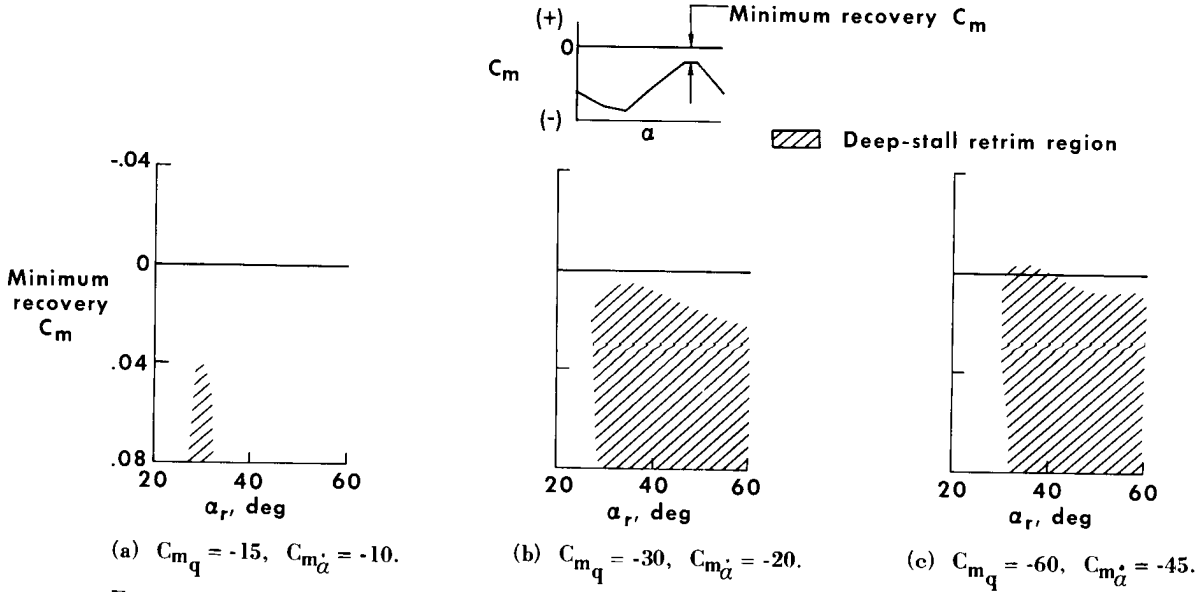


Figure 12.– Deep-stall pitching-moment requirements for recovery from a stall maneuver with an entry rate of 3 knots per second for three levels of damping.

## Effect of Gusts in Causing Pitch-Up

The control-fixed airplane response to half-cycle sine-wave gusts for pitching-moment curves A, D, and E is shown in figures 13 and 14 for trim speeds of $1.3V_S$ and $1.1V_S$, respectively. Also shown in the figures are the sine-wave gust inputs, which had an amplitude of $\alpha_g = 30°$ and periods of 10, 20, and 40 seconds. For $1.3V_S$ and the longer gust periods (fig. 13), the pitch-up region was never encountered as a result of the pitch-down response caused by the large pitch-down region above $\alpha = 10°$

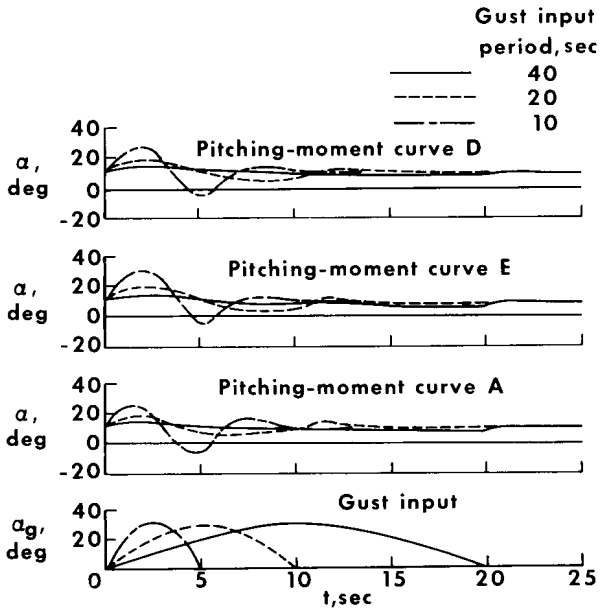


Figure 13.— Response to sinusoidal gust input for trim at $1.3V_S$ ($\alpha = 10°$).

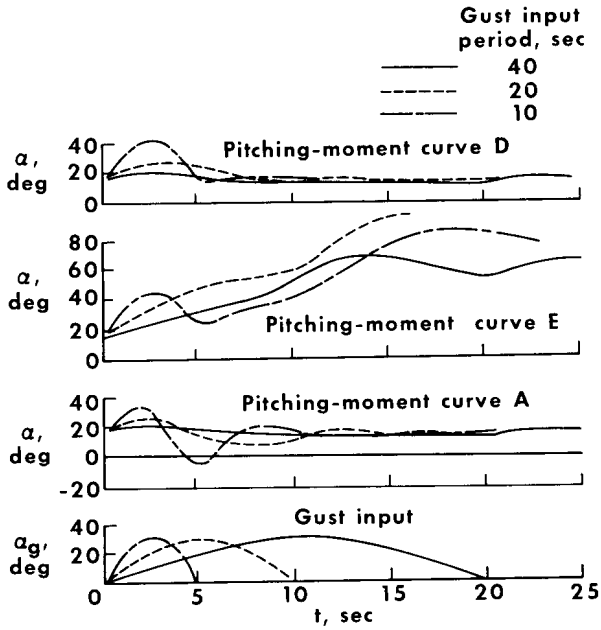


Figure 14.— Response to sinusoidal gust input for trim at $1.1V_S$ ($\alpha = 14°$).

(fig. 1(a)). For the low-period gust input, the pitch-up region was not encountered for a sufficiently long time to allow a divergence in angle of attack. When the trim speed was reduced to $1.1V_S$ (fig. 14), for curve D there was still a sufficient pitch-down region to keep the angle of attack below the pitch-up region for the longest gust period. For the shorter gust periods, the pitch-up region was encountered, but the combined effects of the initial pitch-down response tendency and the rapid reduction in the gust input prevented the occurrence of a deep-stall retrim. For curve E, which had a smaller pitch-down region, the angle of attack did not return to the stable region with the three gust inputs, eventually resulting in deep-stall retrim conditions. Since the gust magnitude used represents an extreme gust condition (corresponding to a gust velocity at an altitude of 10,000 feet of 150 ft/sec for $1.1V_S$ and 184 ft/sec for $1.3V_S$), it appears that for normal operating speeds, gust penetration is not likely to cause a pitch-up to the deep-stall region.

To further define the effects of pitching-moment-curve shape at the initial stall on fixed-control airplane response to gusts at low speeds, a range of sizes of the pitch-down region at the initial stall in terms of $\Delta C_m$ and $\Delta\alpha$ (fig. 15(a)) was investigated in a continuous-gust environment. A tape recording of the gust velocities, obtained from a penetration of a thunderstorm (ref. 9), was used. A typical time history of the gust velocity and the airplane angle-of-attack response is shown in figure 15(b). The results are shown in figure 15(c) in terms of the parameters $\Delta C_m$ and $\Delta\alpha$ (size of pitch-down region), and the maximum gust magnitude that could be penetrated without causing a pitch-up to a deep-stall retrim condition. This magnitude is expressed as a percent of the actual full-scale turbulence level of 15.6 feet per second root mean square (ref. 9). The results indicate that the level of gust magnitude that could be penetrated without producing a deep-stall retrim is dependent on both the height $\Delta C_m$ and width $\Delta\alpha$ of the pitch-down region and varies approximately as the square root of the area of the pitch-down region $\sqrt{(\Delta C_m)(\Delta\alpha)}$. As a result, the gust margin cannot be

specified directly in terms of a speed margin (or angle-of-attack margin) but must, instead, be specified in terms of the size of the pitch-down region of the pitching-moment curve between the desired trim point and the deep-stall trim point.

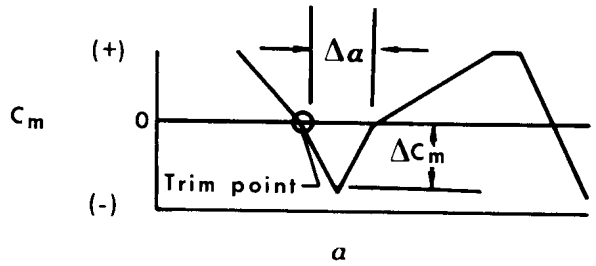


(a) Parameters of pitch-down-region size.

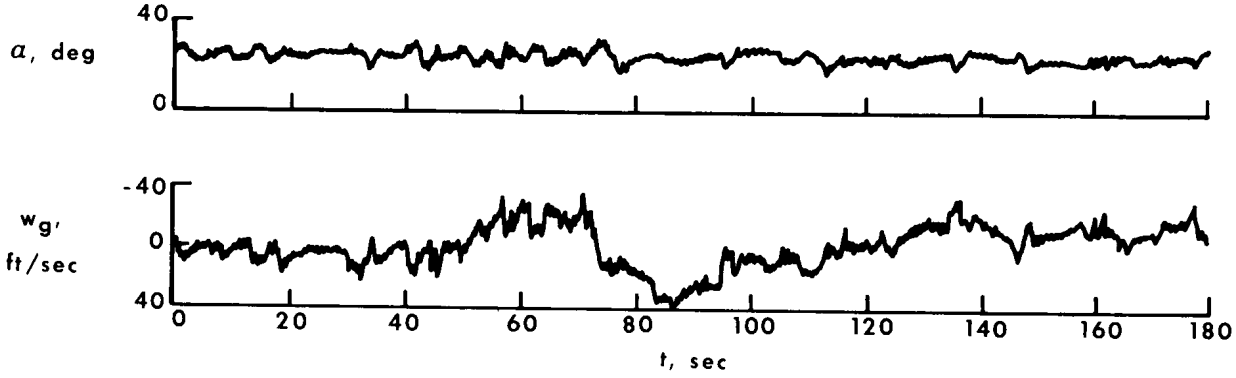


(b) Time history of gust velocity and airplane response; $\Delta\alpha = 8°$, $\Delta C_m = 0.10$, relative gust magnitude = 30 percent.

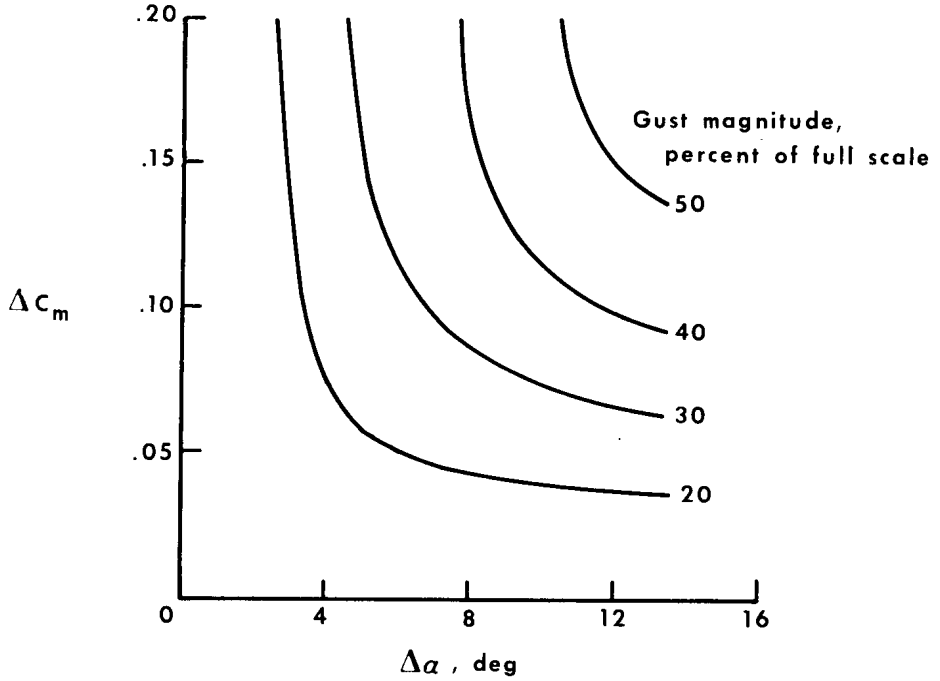


(c) Level of gust magnitude that can be penetrated without causing a pitch-up to a deep-stall retrim.

Figure 15.– Effect of the size of the pitch-down region on preventing pitch-up during continuous-gust penetration.

## CONCLUSIONS

An analog computer program was conducted to study factors that influence the pitch-up characteristics representative of T-tail transport-type aircraft. The results of this study showed that:

1. During a stall maneuver, the time available for a pilot to initiate an acceptable recovery was significantly reduced as the severity of the pitch-up was increased. However, the shape of the pitching-moment curve in the deep-stall region had only a small effect on altitude loss during recovery when recovery initiation was performed as a function of angle of attack.

2. A region of increased stability at the initial stall can be of significant benefit, in that it provides a delay in the occurrence of pitch-up and an increase in control forces required at the initial stall. Both of these factors provide cues that aid the pilot in recognizing the stall condition and afford him additional time to initiate recovery.

3. For a pitching-moment curve with a deep-stall trim point, a recovery is possible if a small amount of pitch-down recovery moment is available throughout the deep-stall region when light damping is present.

4. A pitch-down region at the initial stall provided a margin to prevent pitch-up caused by gust penetration. The margin varied approximately as the square root of the area under the curve of pitch-down moment versus angle of attack.

Flight Research Center,
National Aeronautics and Space Administration,
Edwards, Calif., March 28, 1966.

## REFERENCES


1. Campbell, George S.; and Weil, Joseph: The Interpretation of Nonlinear Pitching Moments in Relation to the Pitch-Up Problem. NASA TN D-193, 1959.

2. Holleman, Euclid C.; and Boslaugh, David L.: A Simulator Investigation of Factors Affecting the Design and Utilization of a Stick Pusher for the Prevention of Airplane Pitch-Up. NACA RM H57J30, 1958.

3. Sadoff, Melvin; Stewart, John D.; and Cooper, George E.: Analytical Study of the Comparative Pitch-Up Behavior of Several Airplanes and Correlation With Pilot Opinion. NACA RM A57D04, 1957.

4. Ray, Edward J.; and Taylor, Robert T.: Effect of Configuration Variables on the Subsonic Longitudinal Stability Characteristics of a High-Tail Transport Configuration. NASA TM X-1165, 1965.

5. White, Maurice D.; and Cooper, George E.: Simulator Studies of the Deep Stall. Conference on Aircraft Operating Problems, NASA SP-83, 1965, pp. 101-110.

6. Taylor, Robert T.; and Ray, Edward J.: Deep-Stall Aerodynamic Characteristics of T-Tail Aircraft. Conference on Aircraft Operating Problems, NASA SP-83, 1965, pp. 113-121.

7. Taylor, Robert T.; and Ray, Edward J.: A Systematic Study of the Factors Contributing to Post-Stall Longitudinal Stability of T-Tail Transport Configurations. Paper No. 65-737, AIAA, 1965.

8. Lina, Lindsay J.; and Moul, Martin T.: A Simulator Study of T-Tail Aircraft in Deep Stall Conditions. Paper No. 65-781, AIAA, 1965.

9. Steiner, Roy; and Rhyne, Richard H.: Some Measured Characteristics of Severe Storm Turbulence. Rep. No. 10, National Severe Storms Project, U. S. Dept. of Commerce, July 1962.